



Dynamic Response of the Airliner Tail Structure During UAS Airborne Collision

Yulong Li

School of Civil Aviation, Northwestern Polytechnical University, Xi'an China
Shaanxi Key Laboratory of Impact Dynamics and Its Engineering Application





CONTENT

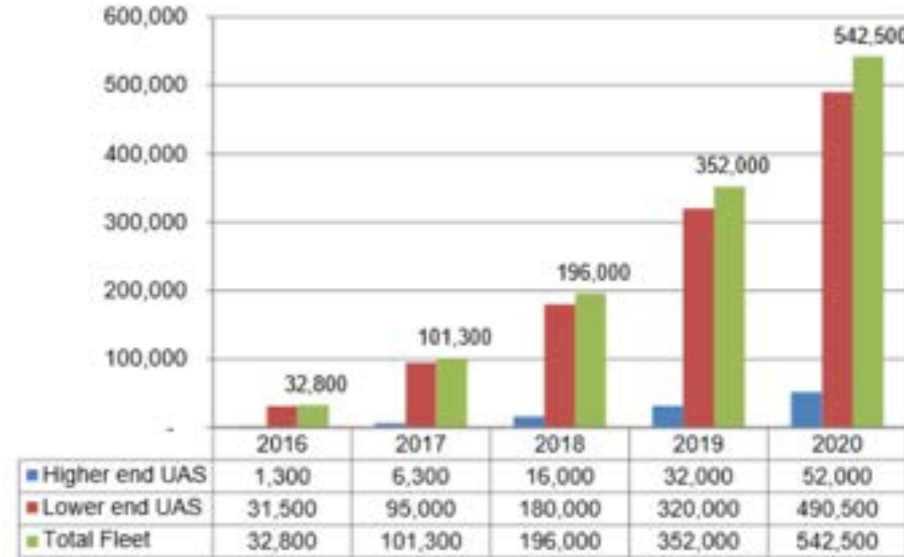
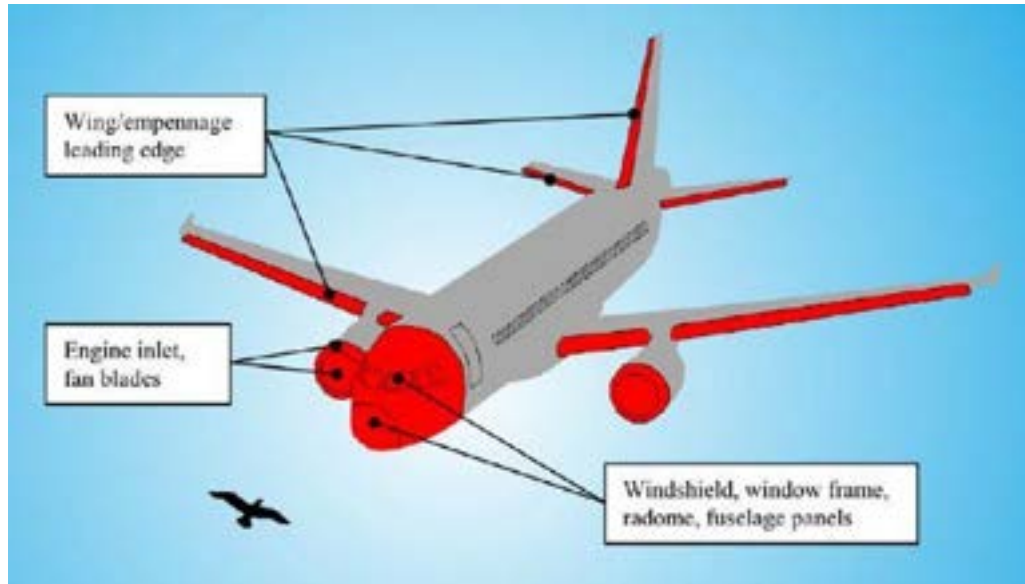
- 1. Motivation & Background**
- 2. Description of the FE Model**
- 3. Experimental Validation**
- 4. Discussion of Different Impact Scenarios**
- 5. Comparison with Bird Strike**
- 6. Conclusion**



PART.1 Motivation & Background



Motivation & Background



The AUVSI forecast that the UAS market volume will reach 4.7 million units by 2020



Bird strike



Hail strike



737 was hit by a drone during the landing process (17th Nov. 2017)

Motivation & Background

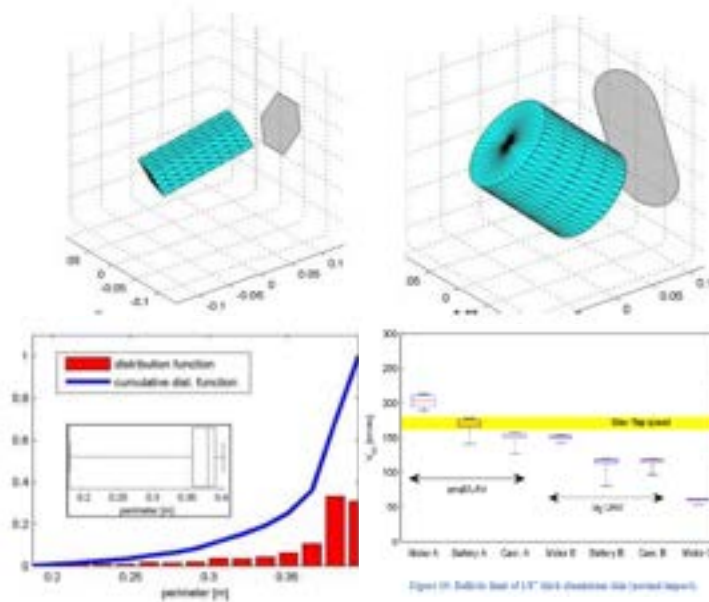
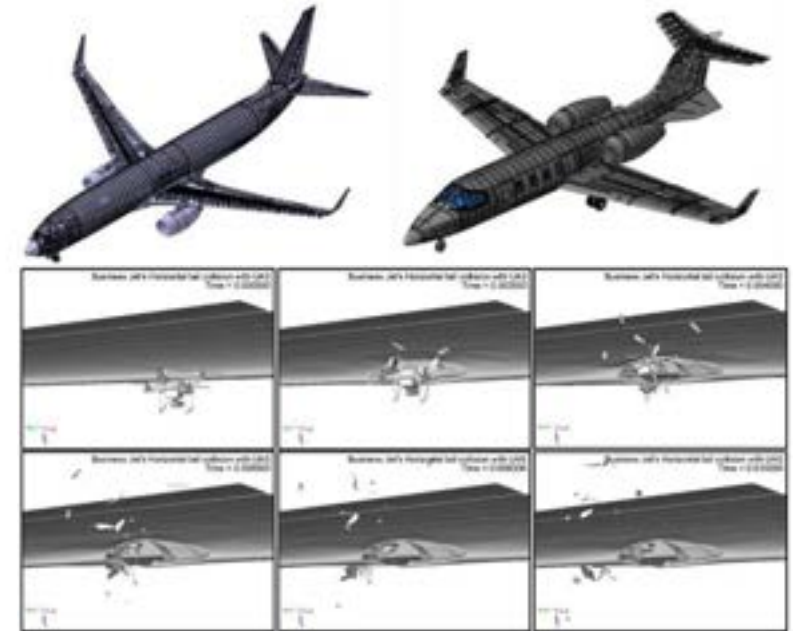


Figure 1: Airliner cockpit for impact testing (left) and computer reference model



Figure 2: 4 kg class drone components model



Potential damage assessment mid air collision small RPA (Australia, 2013)

Small remotely piloted aircraft systems drones mid air collision study (U.K. 2016)

UAS Airborne Collision Hazard Severity Evaluation (ASSURE, 2017)

This work:

Structural level drone collision ground test in accordance with **real collision scenario**.

Finite element model obtained through reverse engineering and **validated by structural level test data**.

Hazard assessment of different drone airborne collision scenarios by validated computational model.

PART.2 Description of the FE Model



Description of the FE Model

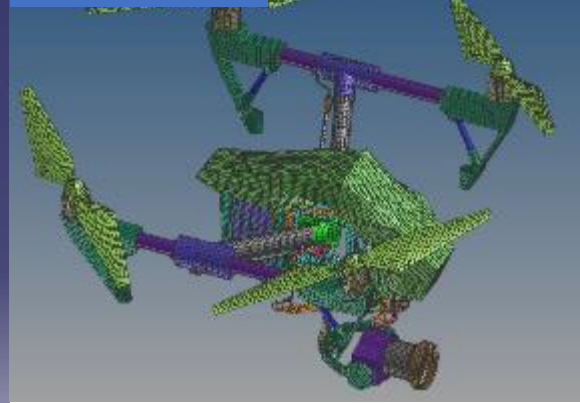
Inspire I



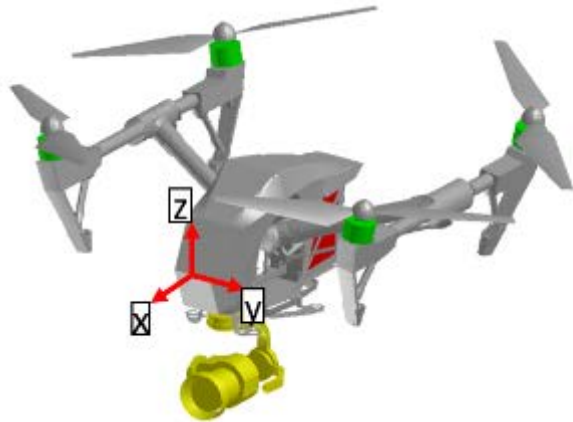
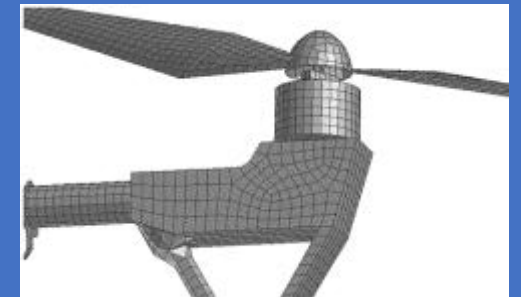
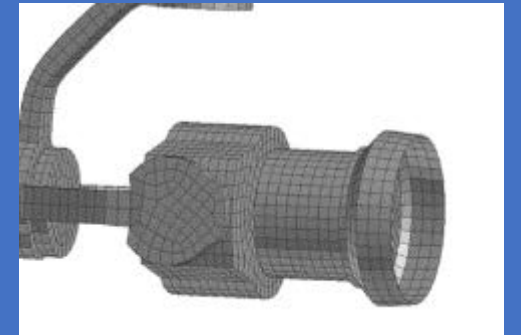
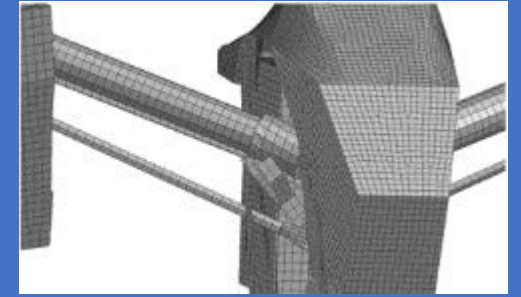
CAD model






FE model



Average mesh size: 5mm



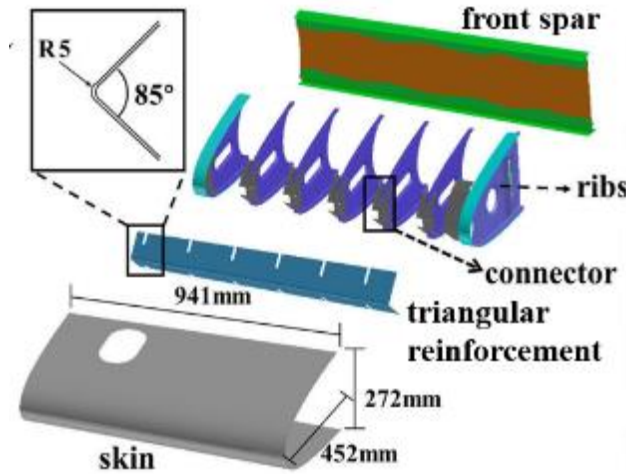
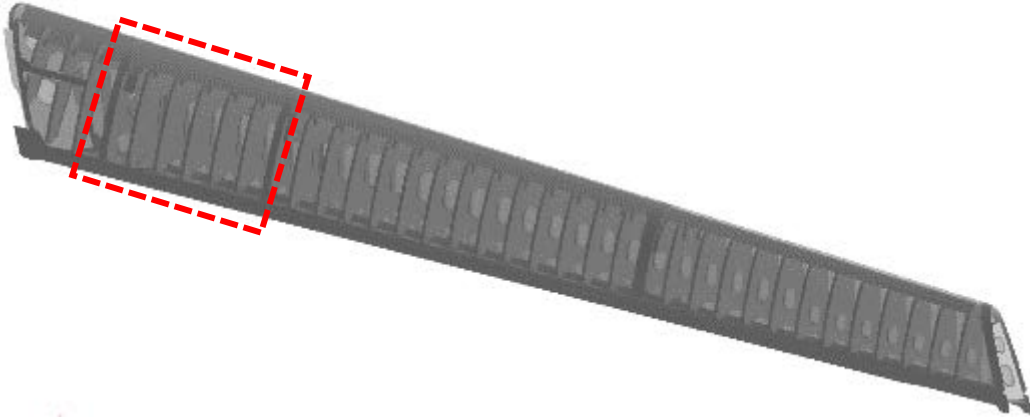
Component	Mass/kg	Center of gravity/mm
Total UAS	3.428	(-197, 0, 5)
 motors	0.462	(-214, 0, 12)
 battery	0.57	(-271, 0, 4)
 camera	0.64	(-125, 0, -161)

Shell elements:
22971

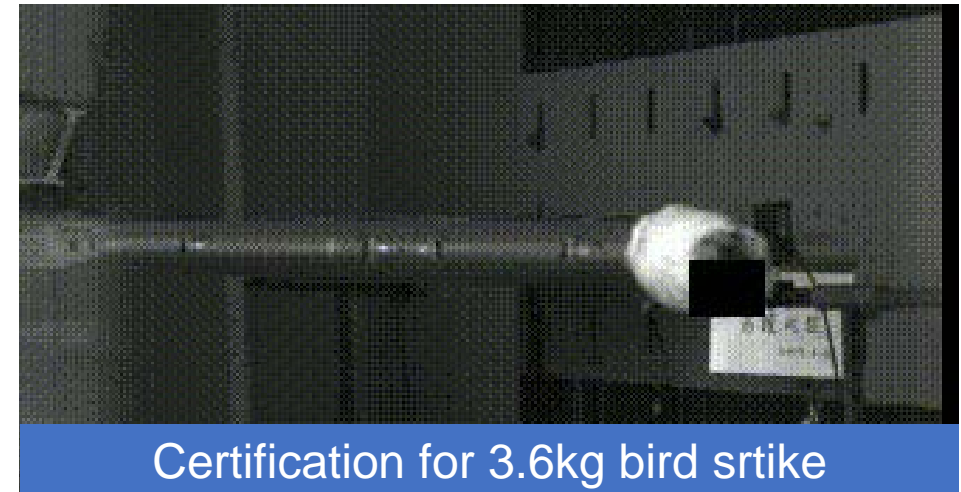
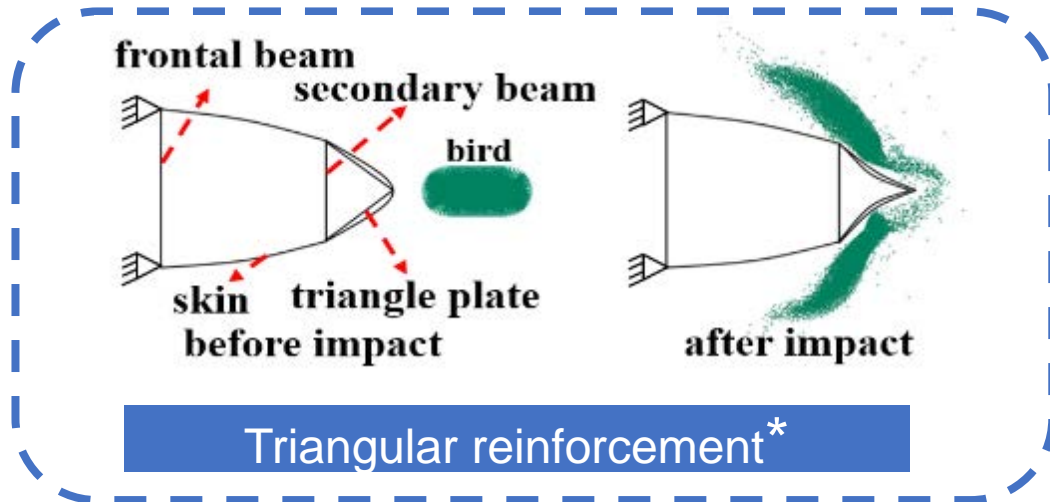
Solid elements:
11544

Description of the FE Model

Airliner horizontal stabilizer leading edge



Code	Material	Thickness
	2024-T3	1.2-2mm
	7075-T6	1.27mm
	7075-T6	1.27mm
	7075-T6	1mm+1mm
	7075-T6	1.6mm
	7075-T6	2mm
	7075-T6	1.27mm

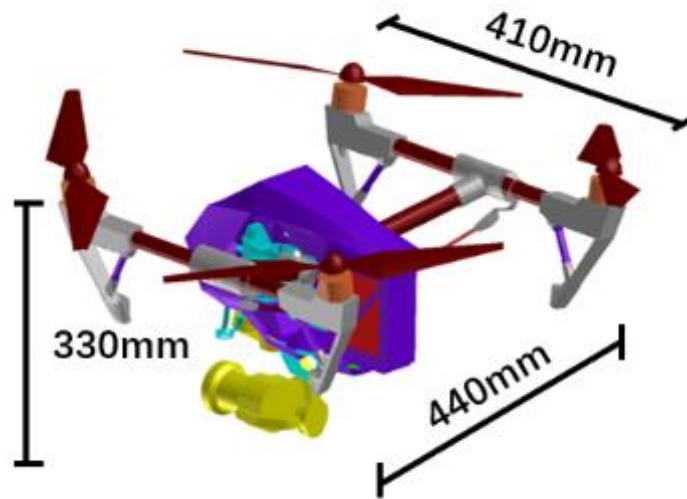


Certification for 3.6kg bird strike

* Jun Liu et al. International Journal of Impact Engineering, 2017

Description of the FE Model

Drone material model



Code	Material
	Polycarbonate
	Polyamide 6
	Carbon Fiber Reinforced Polymer
	battery
	camera
	6061-T6 aluminum alloy
	electronic boards
	motor

PC and PA6

	Density	Young modulus	Poisson's ratio	Yield stress	Failure strain
	ρ [kg/m ³]	E [GPa]	ν	σ_y [MPa]	ϵ_{max}
PC	1180	2.35	0.3	62	0.2
PA6	1350	6.2	0.3	70	0.2

CFRP

Young's modulus	Young's modulus	Poisson's ratio	Shear modulus
E_1 [GPa]	E_2 [GPa]	ν_{12}	G_{12} [GPa]
191	9.9	0.33	6.3

Lithium-ion battery

Density	Young modulus	Poisson's ratio
ρ [kg/m ³]	E [MPa]	ν
1750	500	0.01

CFRP damage evolution

$$E_1 = \begin{cases} E_1^0 & \epsilon_{11} < \epsilon_i^f \\ E_1^0(1-d^f); \quad d^f = d_u^f \frac{\epsilon_{11} - \epsilon_i^f}{\epsilon_u^f - \epsilon_i^f} & \epsilon_i^f \leq \epsilon_{11} < \epsilon_u^f \\ E_1^0(1-d^f); \quad d^f = 1 - (1-d_u^f) \frac{\epsilon_{11}}{\epsilon_u^f} & \epsilon_u^f \leq \epsilon_{11} \end{cases}$$

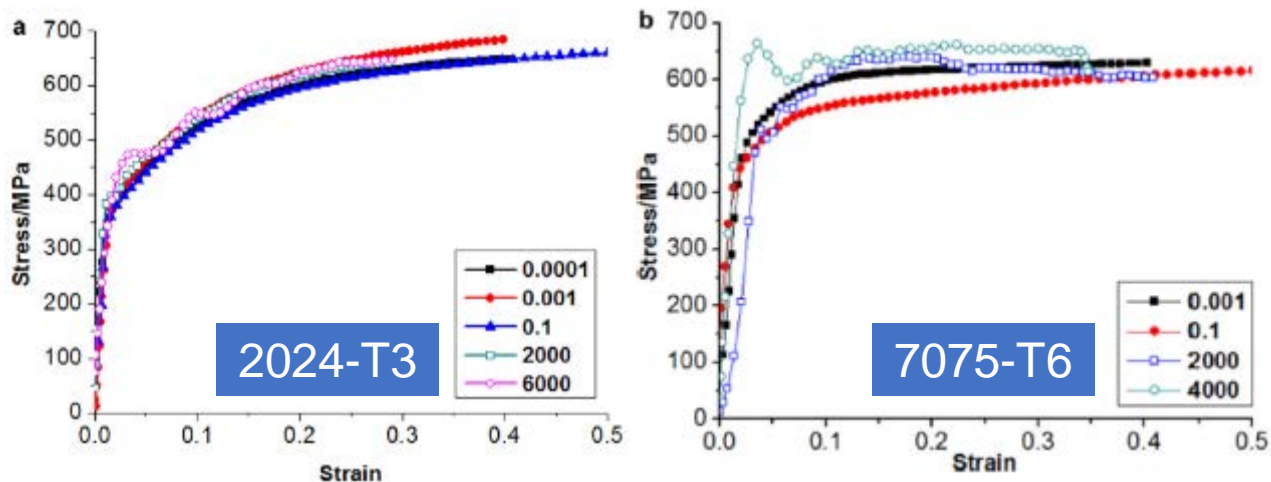
$$\begin{cases} Y = \sqrt{\frac{1}{2} \frac{\sigma_{12}^2 + \sigma_{13}^2}{G_{12}}} + b \frac{1}{2} \frac{\langle \sigma_{22} \rangle^2}{E_2} & \text{(shear damage)} \\ Y' = \sqrt{\frac{1}{2} \frac{\langle \sigma_{22} \rangle^2}{E_2}} & \text{(transverse damage)} \end{cases}$$

$$\begin{cases} d = \langle Y - Y_0 \rangle / Y_c & \text{(shear damage)} \\ d' = \langle Y - Y'_0 \rangle / Y'_c & \text{(transverse damage)} \end{cases}$$

$$\begin{cases} E_2 = E_2^0(1-d') \\ G_{12} = G_{12}^0(1-d) \end{cases}$$

Description of the FE Model

Aluminum alloy



Johnson-Cook Model $\sigma = (A + B\varepsilon^n)(1 + C \ln \dot{\varepsilon}^*)(1 - (T^*)^m)$

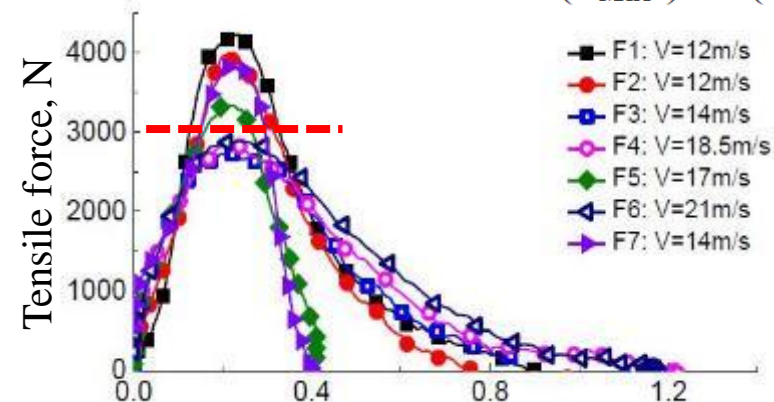
Parameters of aluminum alloy

	A [MPa]	B [MPa]	n	C	ε_{\max}
2024-T3	280	400	0.2	0.015	0.2
7075-T6	480	400	0.42	-0.001	0.12

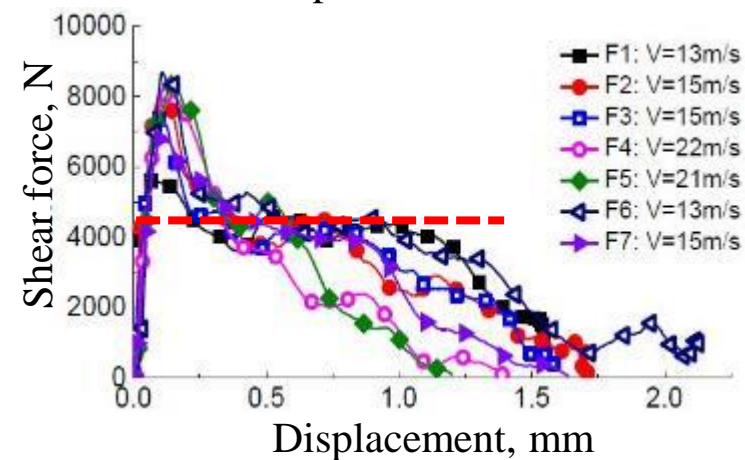
Fastener (P-LINK element)

Rupture model

$$\left(\frac{T}{T_{MAX}}\right)^n + \left(\frac{S}{S_{MAX}}\right)^m \leq 1$$



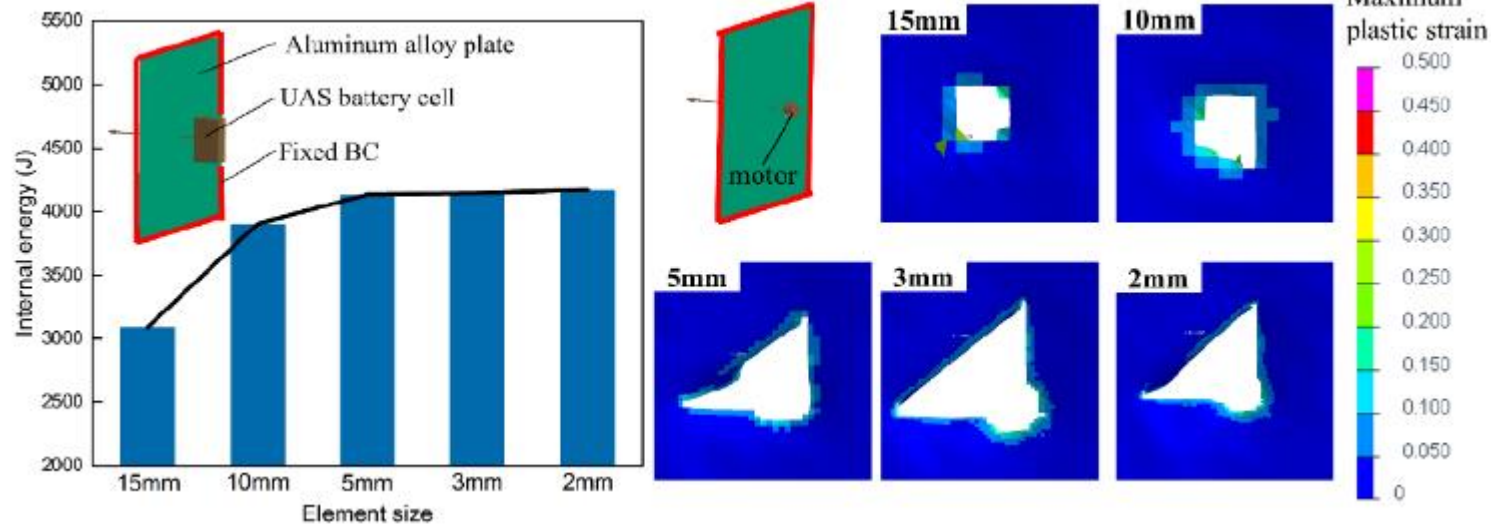
$T_{MAX}=3000N$



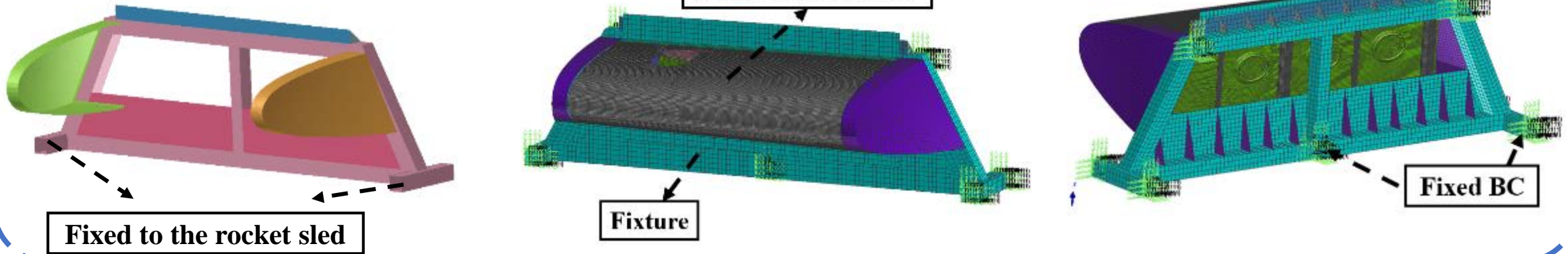
$S_{MAX}=4200N$

Description of the FE Model

Mesh Sensitive Test



Fixture and boundary conditions

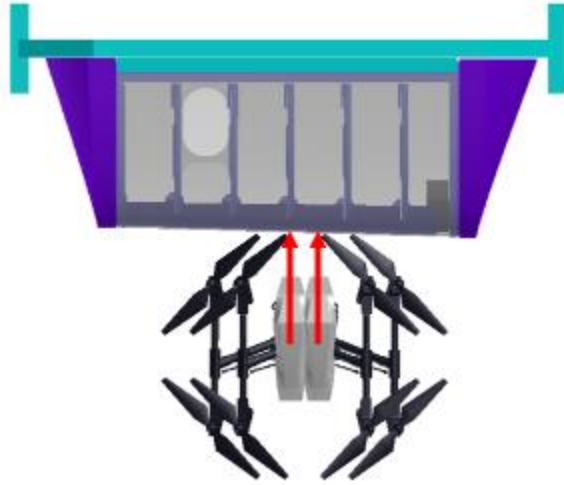


PART.3 Experimental Validation



Experimental Validation

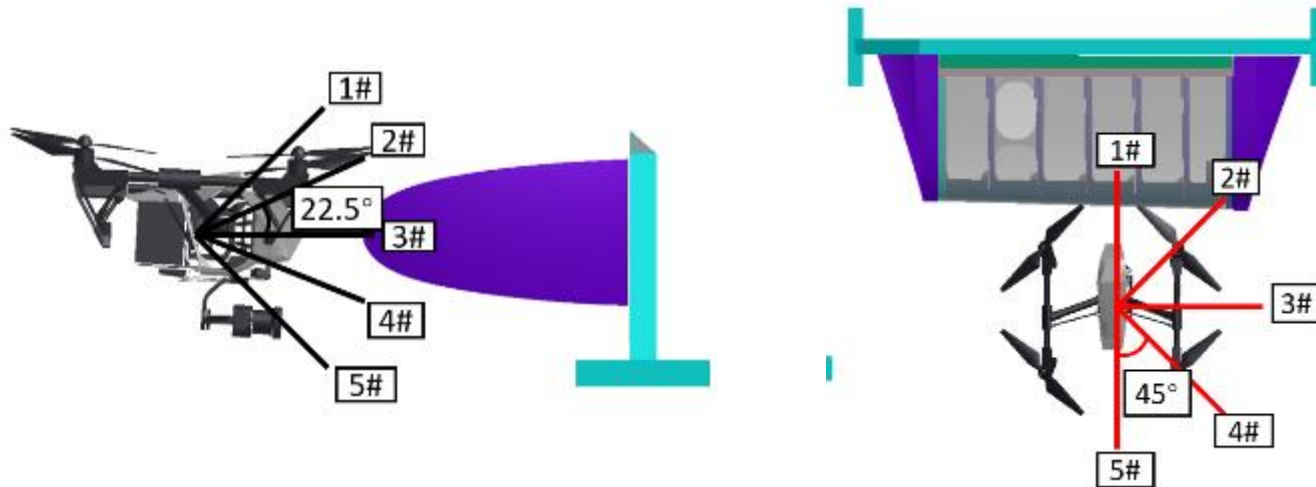
Test collision scenario determination



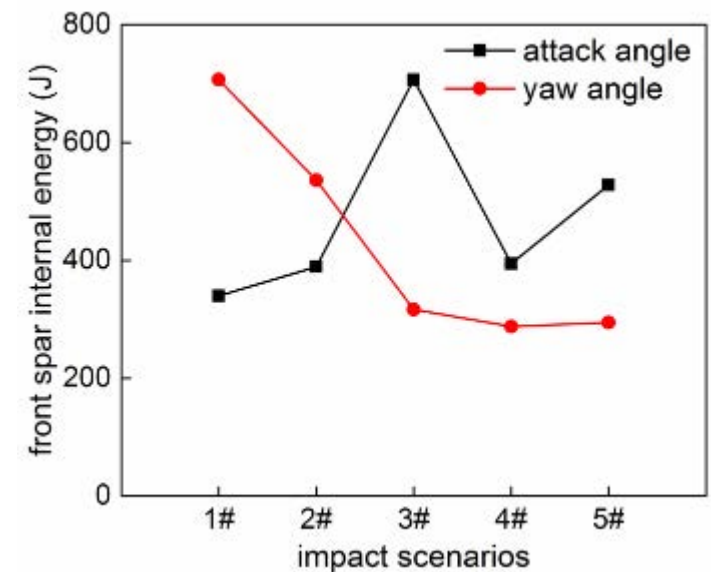
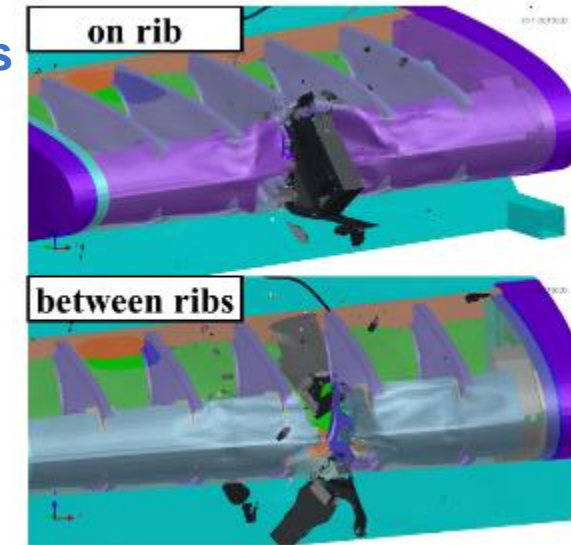
Impact locations:
on rib & between ribs

Drone attack angle:
 $-45^{\circ} \sim 45^{\circ}$ at an interval of 22.5°

Drone yaw angle:
 $1^{\circ} \sim 180^{\circ}$ at an interval of 45°

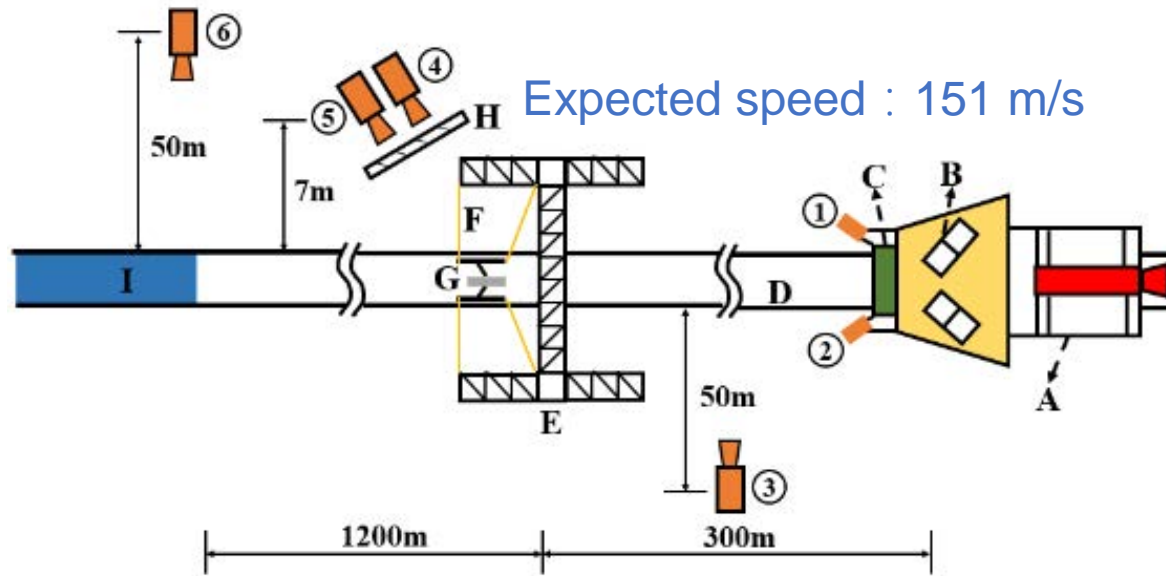


Results

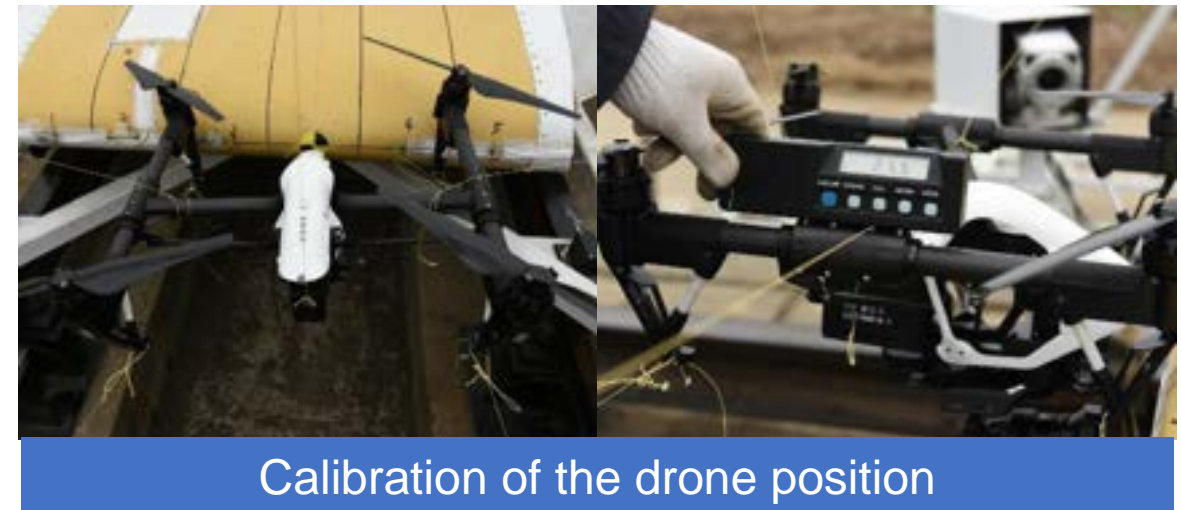
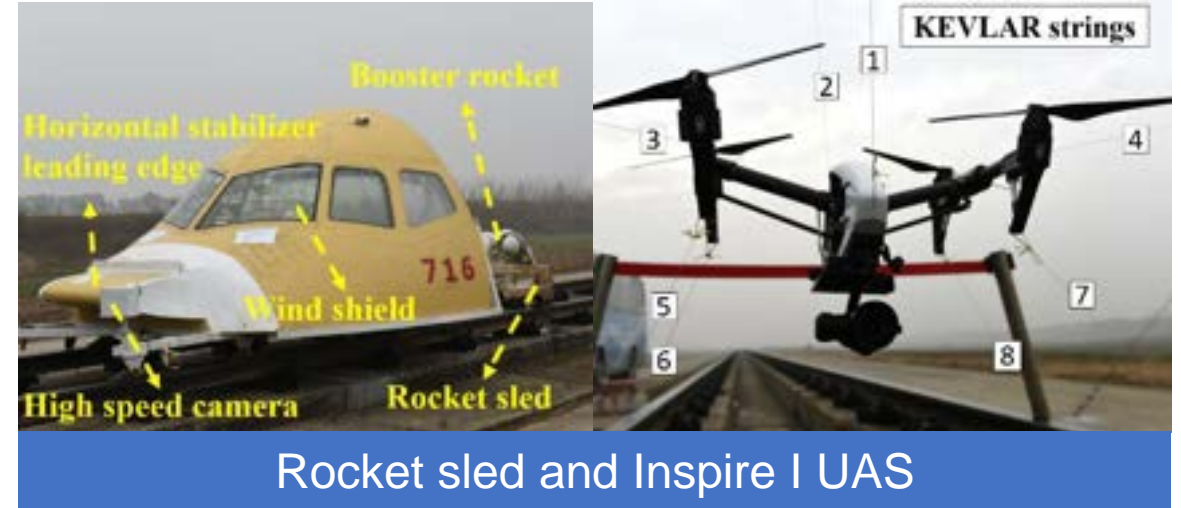


Experimental Validation

Test procedure

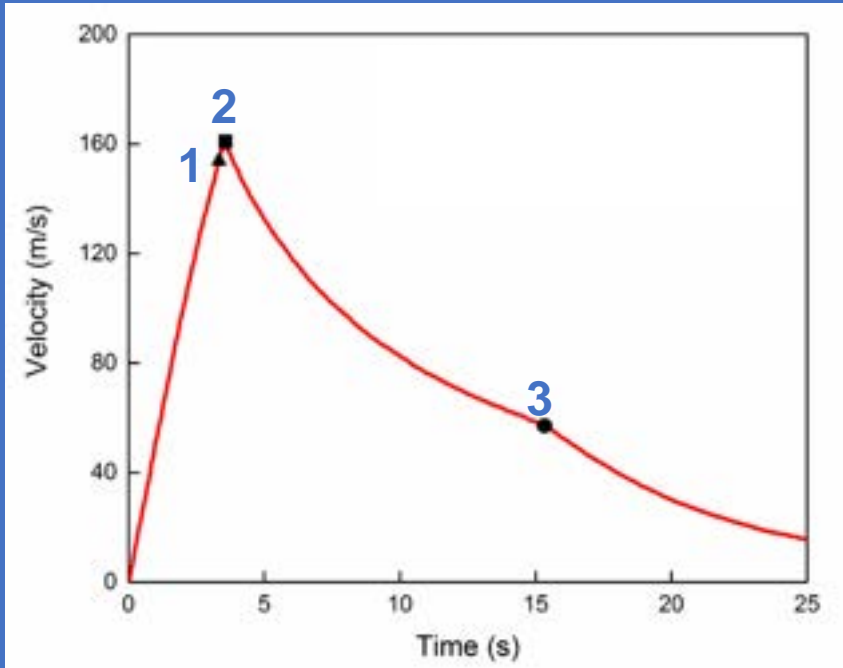


(A) rocket sled, (B) head structure and windshield, (C) horizontal stabilizer leading edge, (D) steel track, (E) fixture frame for the drone, (F) KEVLAR strings, (G) the drone, (H) shield for high-speed cameras, (I) water brake. 1-6 high-speed cameras.



Experimental Validation

Sled velocity



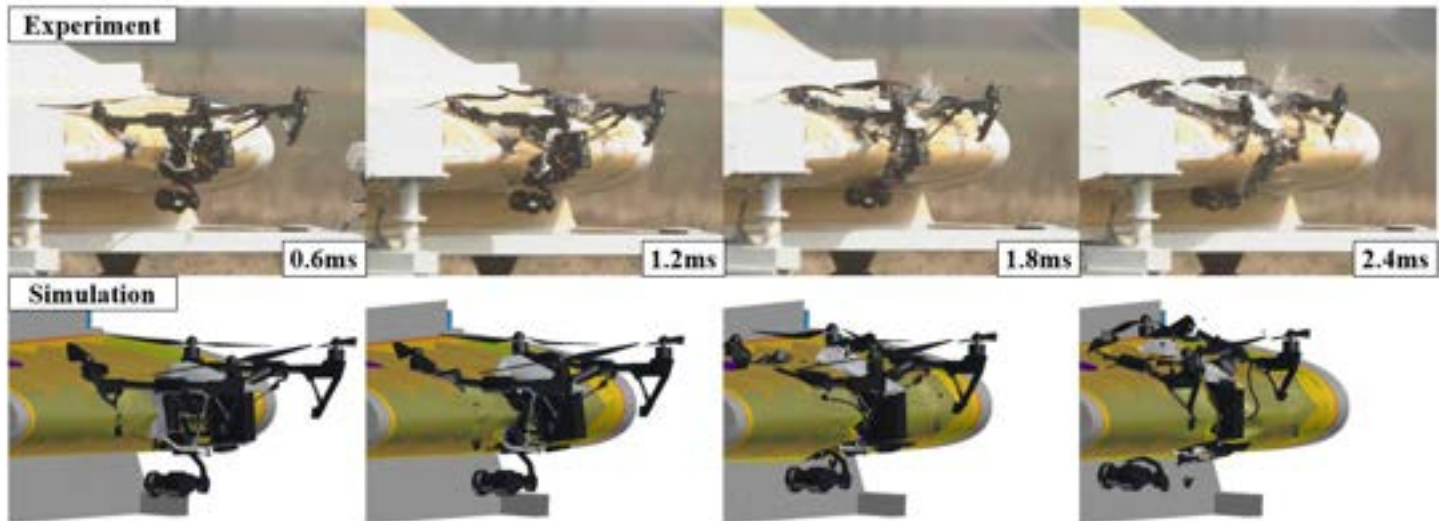
1. Impact point $v=152.8\text{m/s}$
2. Fuel exhaustion $v=159.2\text{m/s}$
3. Water brake $v=56.4\text{m/s}$



High-speed camera 4

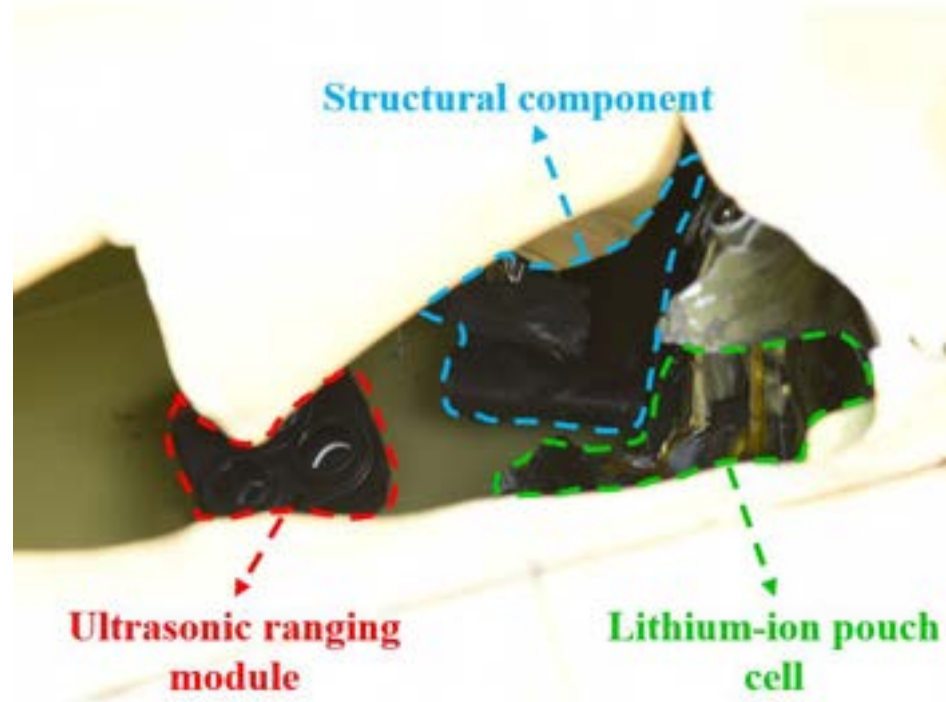
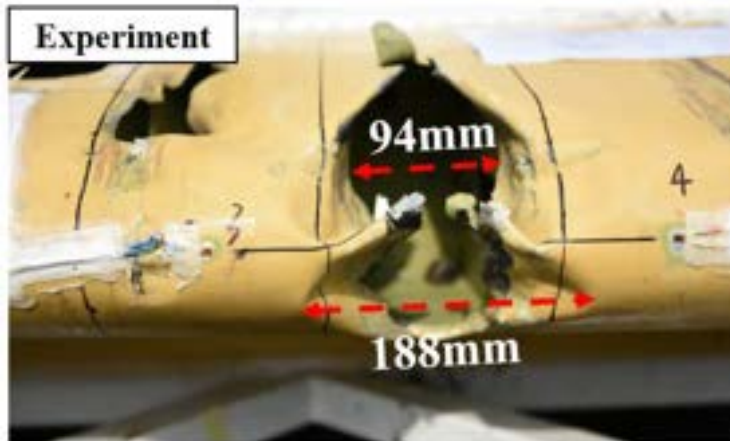


High-speed camera 1



Experimental Validation

Damage features



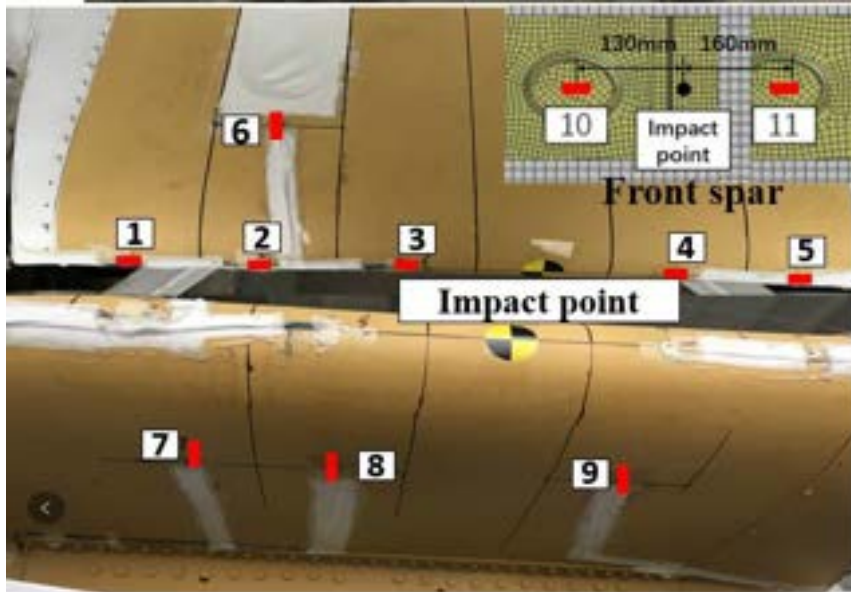
The main structure of the drone penetrated into the airframe

Some small drone components penetrated the front spar (fracture size about 15 mm)

The lithium-ion battery penetrated into the airframe had a smoke sign in the test

Experimental Validation

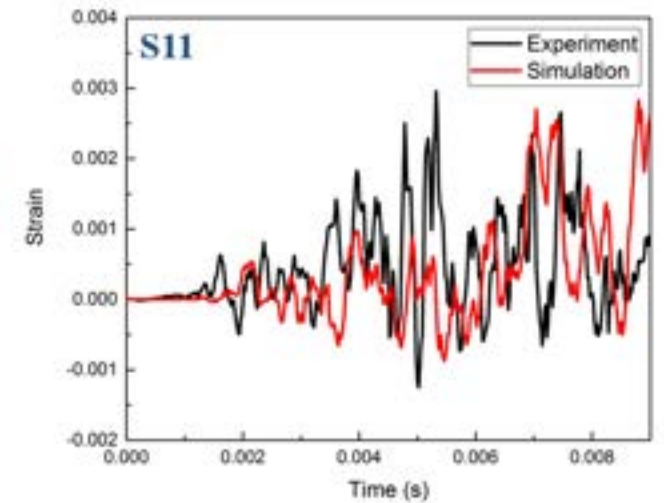
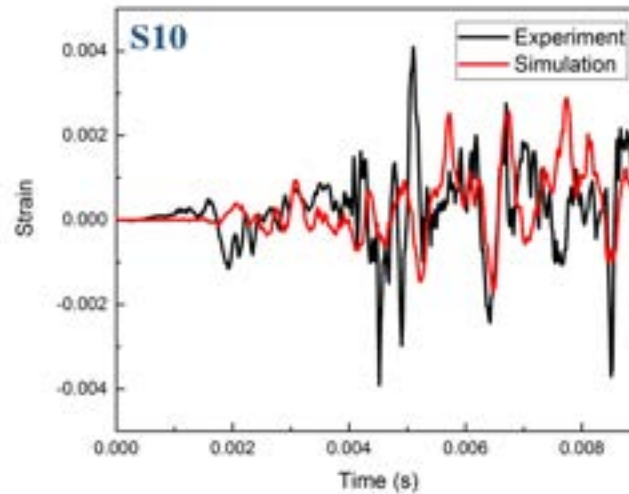
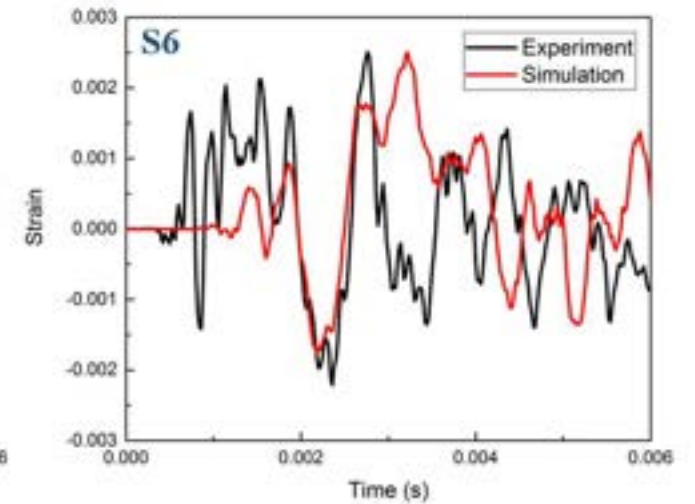
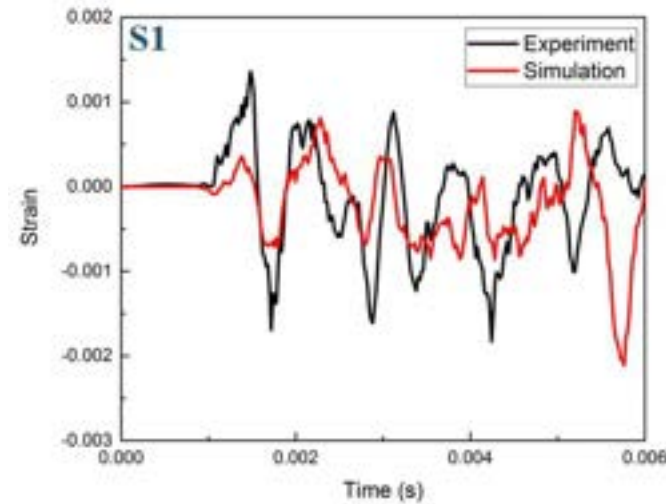
Strain signals



randomness factors during the collision process

the differences between the simplified FE model and real drone structure.

Uncertainty of precise drone posture

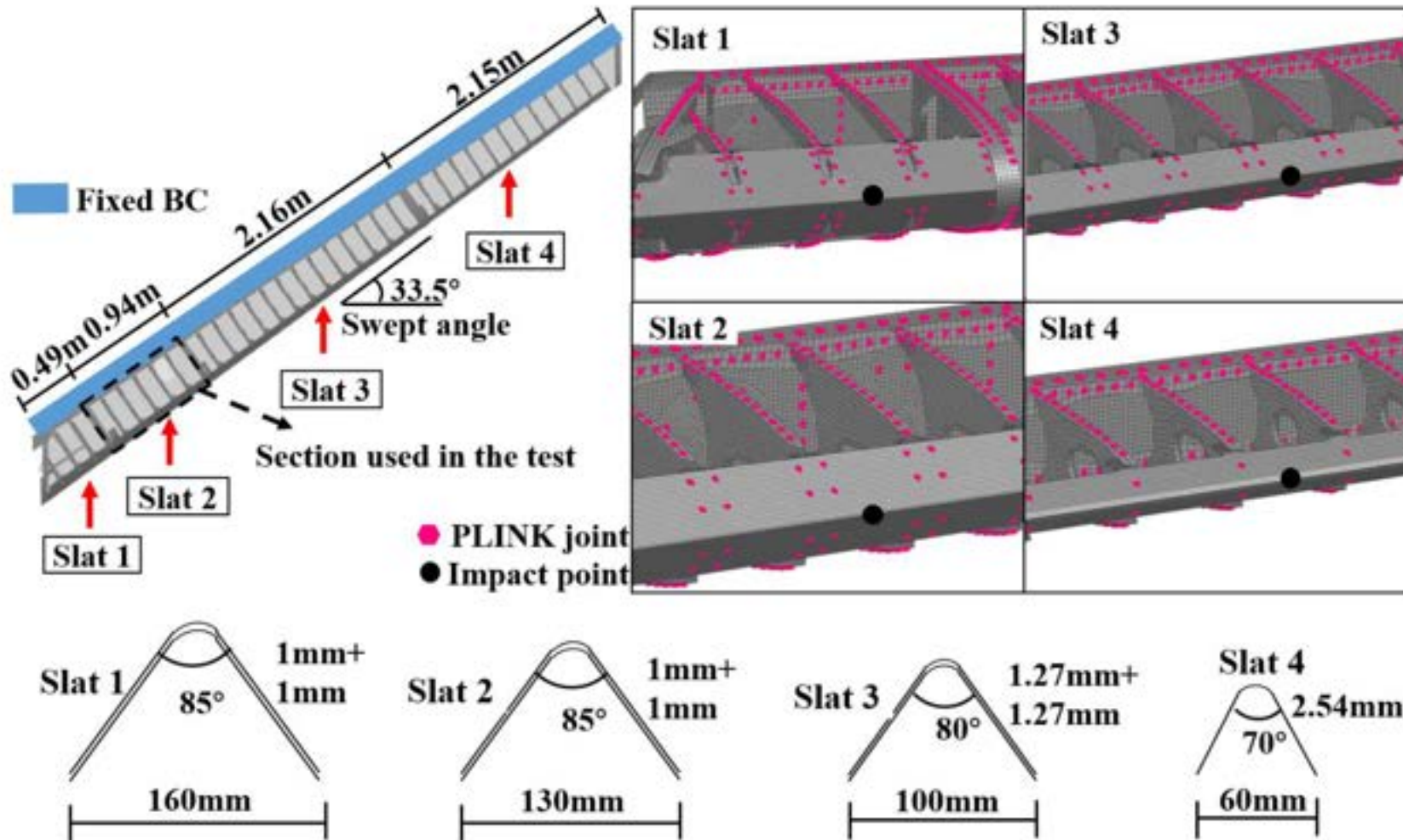


PART.4 Discussion of Different Impact Scenarios



Discussion of Different Impact Scenarios

horizontal stabilizer leading edge FE model



The structure was about 5.74 m long and can be divided into four sections

The whole FE model contained 318,333 shell elements and 3194 PLINK elements.

Fixed boundary conditions were applied on the upper and lower edges of the front spar

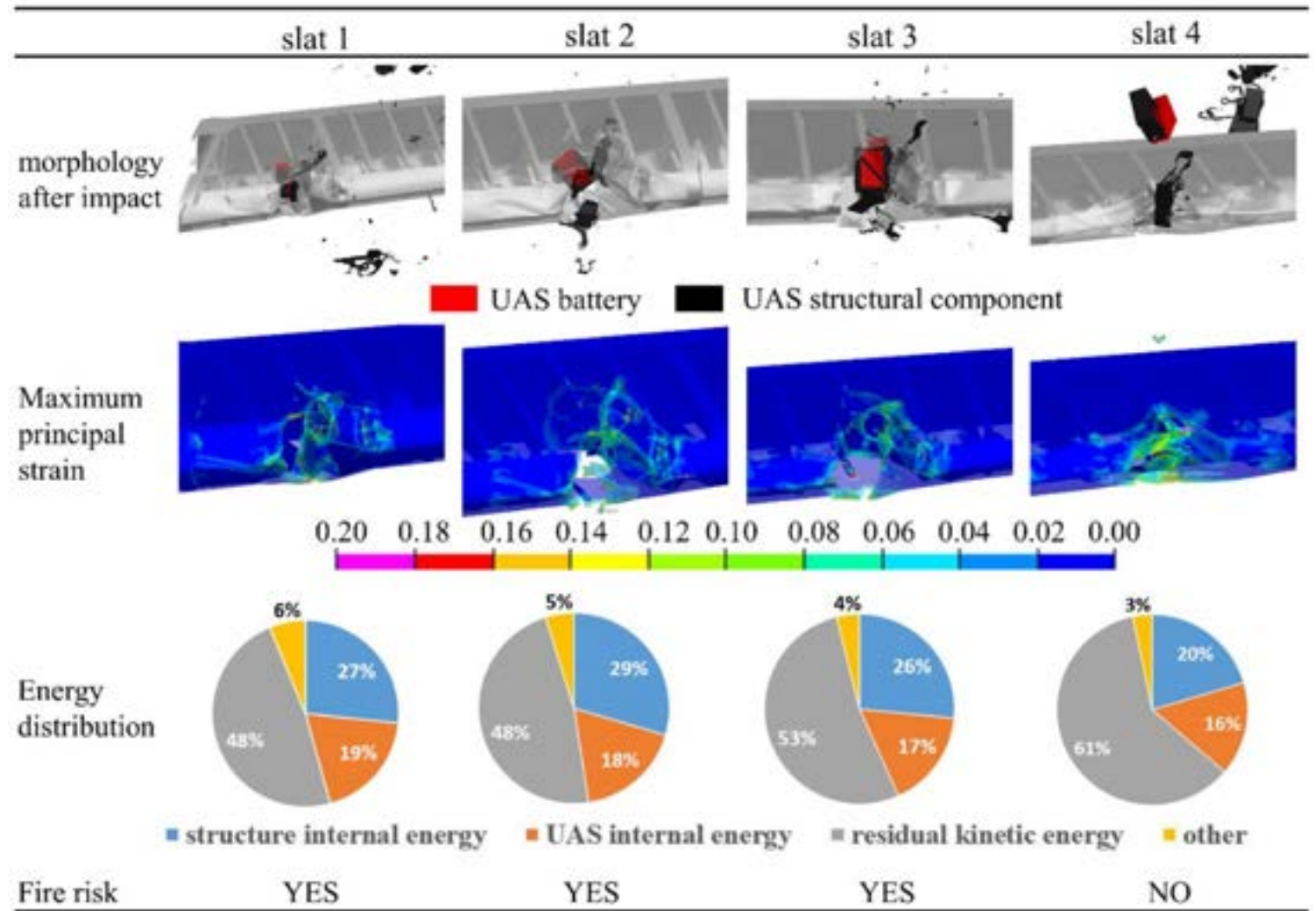
Discussion of Different Impact Scenarios

Different impact locations

Drone projection areas on the leading edge at different impact points

Impact point	Projection area [cm ²]	Projection area [%]	Mass in projection area [kg]	Mass in projection area [%]
Slat 1	358.4	83.9%	2.707	79.0%
Slat 2	341.3	79.9%	2.529	73.8%
Slat 3	295.6	69.2%	2.172	63.4%
Slat 4	190.5	44.6%	1.577	46.0%

Results



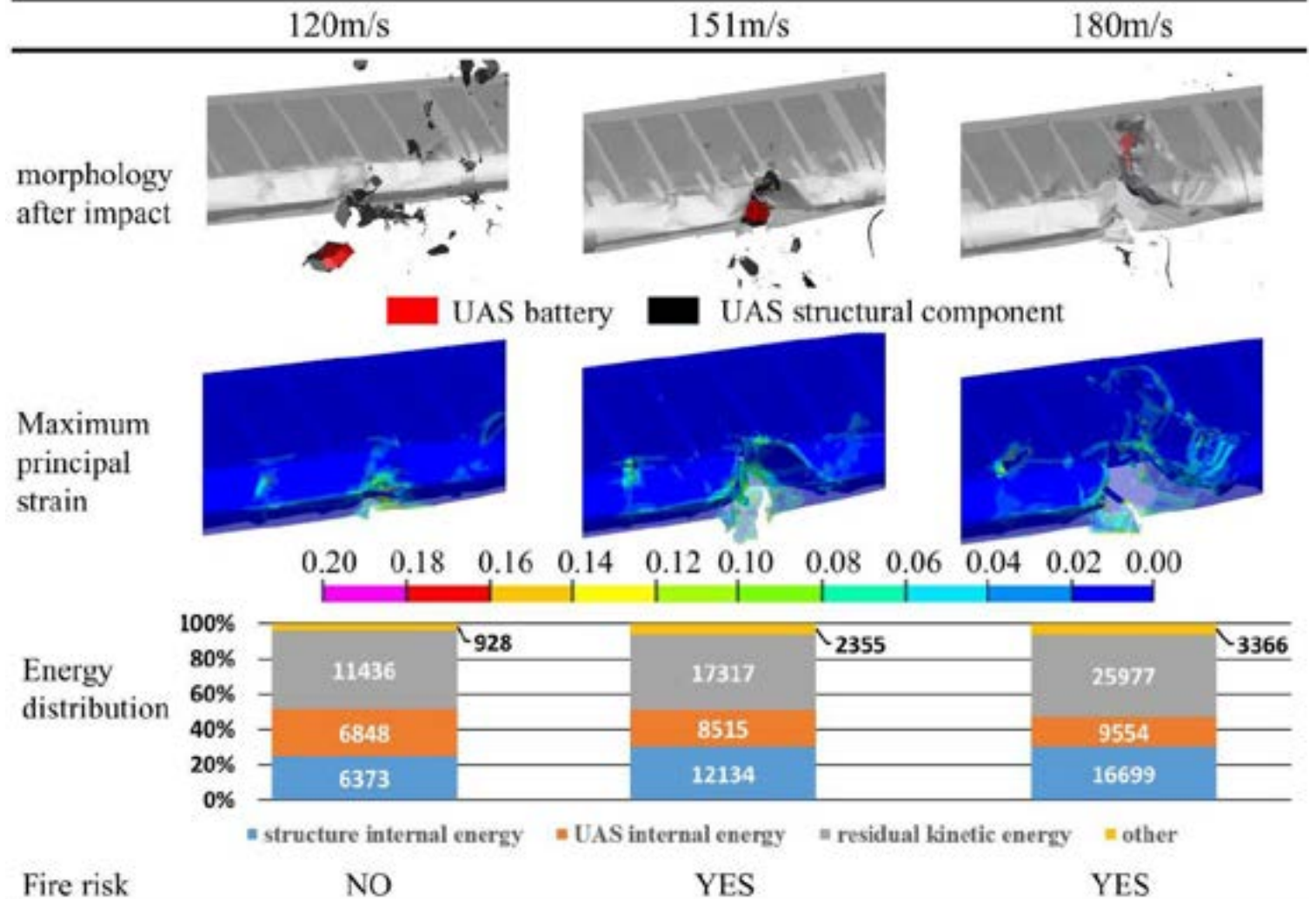
Discussion of Different Impact Scenarios

Different impact locations

Velocity-attack angle relationship of the airliner

Velocity [m/s]	Attack angle [°]	Projection area [%]	Mass in projection area [%]
95	15°	78.4%	76.4%
126	10°	80.9%	78.2%
155	4°	78.7%	78.2%

Results

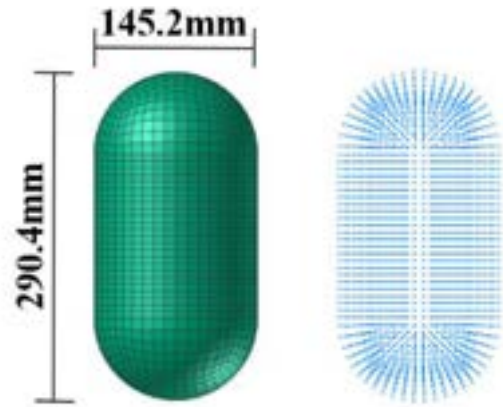


PART.5 Comparison with Bird Strike



Comparison with Bird Strike

Bird model

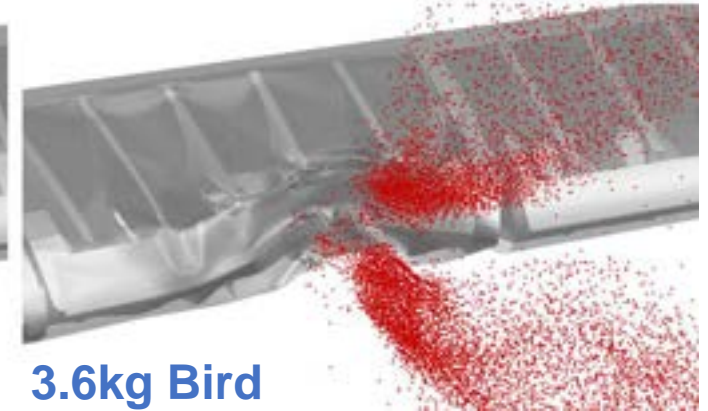


Murnaghan EOS

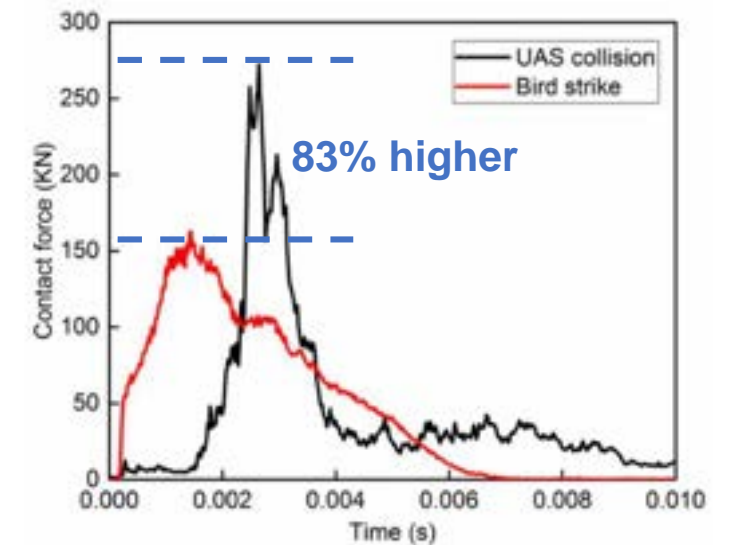
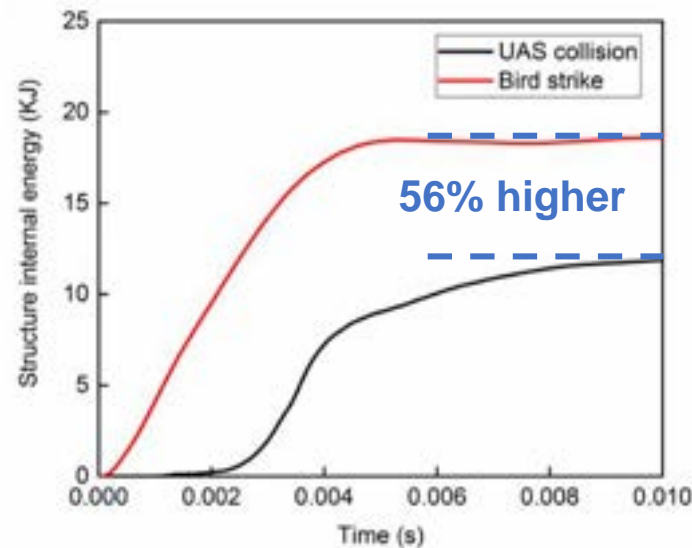
$$p = p_0 + B \left[\left(\frac{\rho}{\rho_0} \right)^\gamma - 1 \right]$$

$$B = 128 \text{ MPa}$$
$$\gamma = 7.99$$

Results



Damage characteristics of UAS collision and bird strike (150m/s)



PART.6 Conclusion



Conclusion

- The impact behavior simulated by the FE model was in acceptable agreement with test data and the simulation methodology is proved to be an efficient way to reduce certification costs.
- The commercial airliner cannot complete the flight safely when a UAS airborne collision happens at its cruising speed.
- Some anti-bird strike designs were proved to be not so efficient against UAS airborne collision, new design principles should be considered.
- UAS collision would cause more serious consequences than bird strike at the same mass level, Relevant airworthiness standards should be drafted.

THANK YOU

ANY QUESTIONS?

- This work was funded by **Airworthiness Certification Center of CAAC** and **Shanghai Aircraft Airworthiness Certification Center of CAAC**
- All the drones used were supplied by **SZ DJI Technology Co., Ltd**

Acknowledgement:

- Shanghai Airworthiness Certification Center of CAAC: Dr. Shunan Dai, Dr. Yingchun Zhang, Dr. Ye Wang, Mr. Zhuguo Zhang, Mr. Yingju Sun
- Beijing Airworthiness Certification Center of CAAC: Mr. Jingyu Yu
- NPU: Mr. Xianghao Meng, Prof. Ju Liu, Prof. Zhongbin Tang, Prof. Tao Suo

